Twisted Bilayer Graphene: Enhanced electron-phonon coupling and superconductivity

Biao Lian

Princeton Center for Theoretical Science, Princeton University

Collaborators:

Zhijun Wang

Andrei Bernevig

Lian, Wang, Bernevig,
arXiv 1807.04382 (2018)

Outline

***Twisted bilayer graphene (TBG)**:*

- *Flat bands, Dirac helicity*
- *Moire electron-phonon coupling*
- *BCS superconductivity & implication on insulator states*

Twisted Bilayer Graphene (TBG)

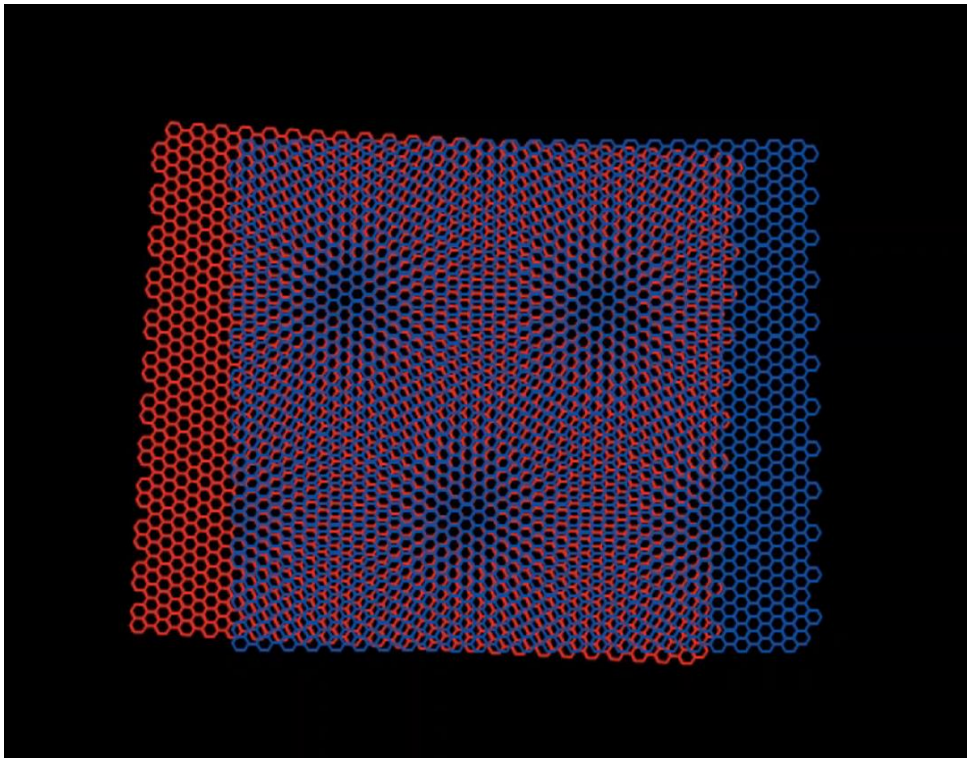

Moire pattern

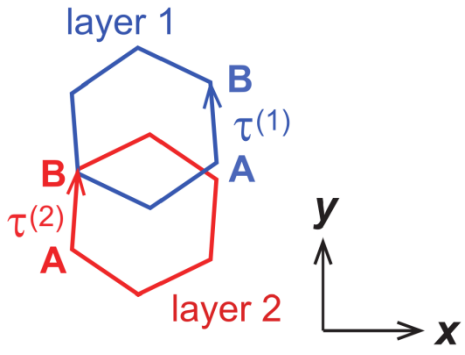

Symmetries:

C_{2x} , C_{6z} ,

time-reversal T

Twisted Bilayer Graphene (TBG) ***superlattice Moire pattern*** (lattice constant $\propto 1/\theta$).

Monolayer Graphene

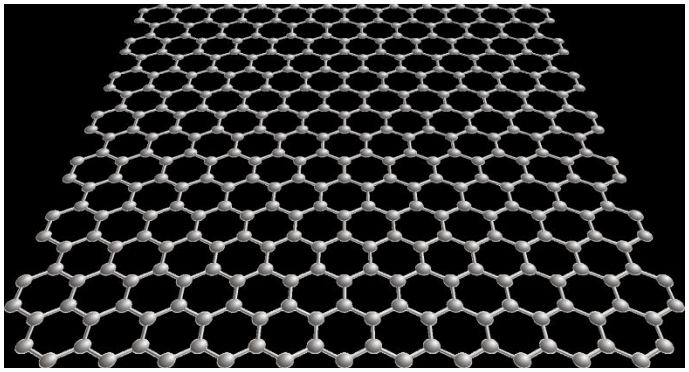

Monolayer Graphene

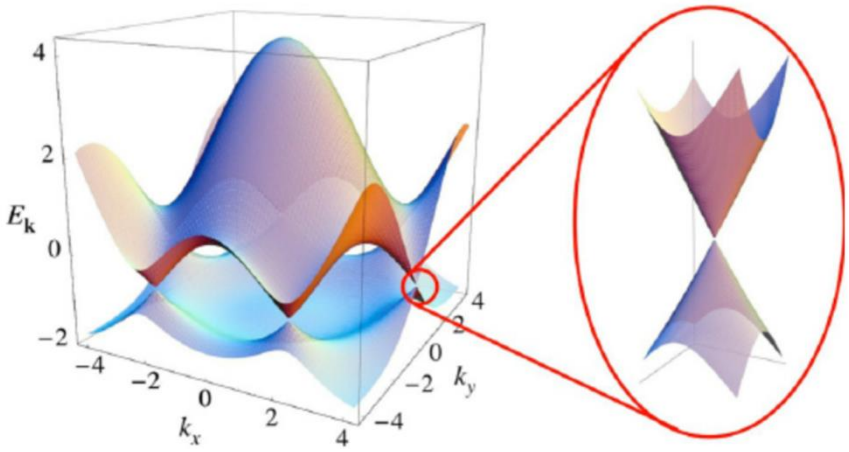

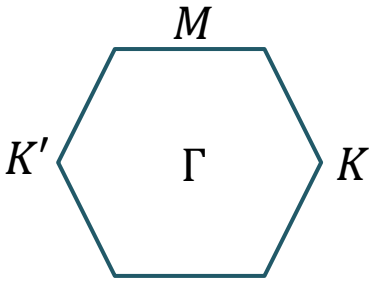

Graphene BZ

Low energy Dirac electrons of monolayer graphene:

Valley K and K' (spin ↑, ↓):

$$\begin{cases} h^{K}(\mathbf{k}) = v(k_x\sigma_x - k_y\sigma_y) = \hbar v\boldsymbol{\sigma}^* \cdot \mathbf{k} & \text{(Helicity } \eta = +1) \\ h^{K'}(\mathbf{k}) = -\hbar v\boldsymbol{\sigma} \cdot \mathbf{k} & \text{(Helicity } \eta = -1) \end{cases}$$

Band structure of TBG

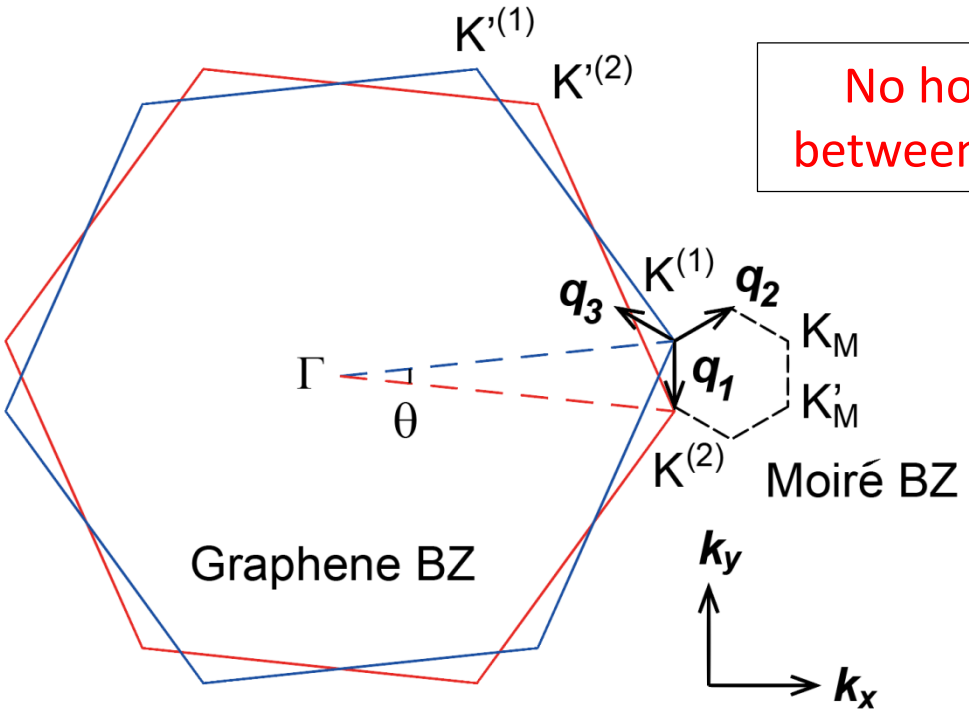

Interlayer electron hopping in momentum $\boldsymbol{k}$ space:

$\boldsymbol{k}$ in layer 1 hop to $\boldsymbol{k} - \boldsymbol{q}_j$ in layer 2 $(j = 1,2,3)$.

Bistritzer, Macdonald (2011)

Band structure of TBG

TBG continuum model at graphene valley K:

$$H^K(\boldsymbol{r}) = \begin{pmatrix} h^K_{\theta/2}(-i\nabla) & w(T_1 e^{i\boldsymbol{q}_1\cdot\boldsymbol{r}} + T_2 e^{i\boldsymbol{q}_2\cdot\boldsymbol{r}} + T_3 e^{i\boldsymbol{q}_3\cdot\boldsymbol{r}}) \\ w(T_1 e^{-i\boldsymbol{q}_1\cdot\boldsymbol{r}} + T_2 e^{-i\boldsymbol{q}_2\cdot\boldsymbol{r}} + T_3 e^{-i\boldsymbol{q}_3\cdot\boldsymbol{r}}) & h^K_{-\theta/2}(-i\nabla) \end{pmatrix}$$

Dirac electron at K_M & K'_M points:

$$\widetilde{H}(\boldsymbol{k}) = \begin{cases} \frac{1-3\alpha^2}{1+6\alpha^2}\hbar v\boldsymbol{\sigma}^*\cdot\boldsymbol{k}\,, & \text{(Graphene valley } K\text{)} \\ -\frac{1-3\alpha^2}{1+6\alpha^2}\hbar v\boldsymbol{\sigma}\cdot\boldsymbol{k}\,, & \text{(Graphene valley } K\text{')} \end{cases}$$

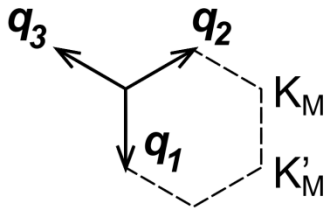

Moiré BZ

$$\alpha = \frac{w}{\hbar v k_\theta}\,,$$
$$k_\theta = |\boldsymbol{q}_j| = \frac{8\pi\sin\theta/2}{3a_0}$$

The ***first Magic angle***: $\alpha^2 = 1/3$, → $\theta \approx 1.05°$.

Bistritzer, Macdonald (2011)

Magic angle & flat band

Moire band structure at $\theta = 1.05°$ (*one graphene valley, one spin*):

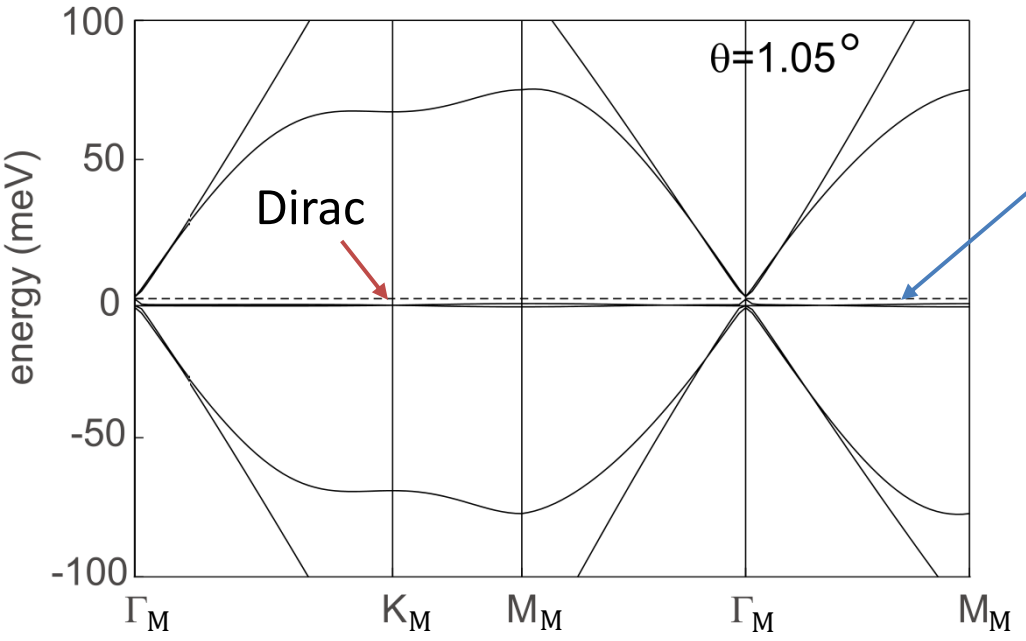

Two flat bands

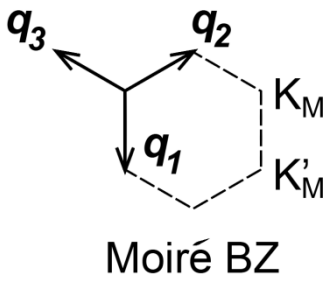

Moiré BZ

All the Moire bands are ***4-fold degenerate*** (graphene valley K, K' and spin ↑ , ↓).

Nonzero Dirac helicity & fragile topology

Graphene valley K

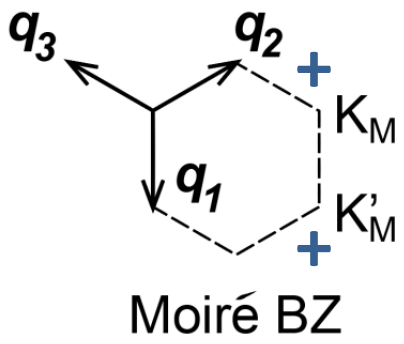

Graphene valley K'

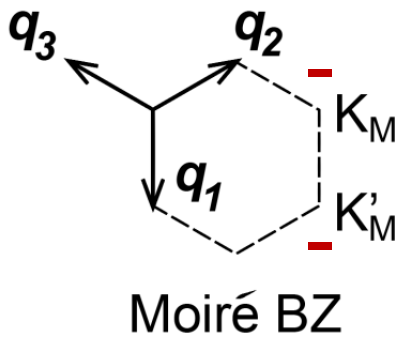

Dirac helicity only depends on graphene valley K, K':

+: $\tilde{H} \propto \boldsymbol{\sigma}^* \cdot \boldsymbol{k}$

-: $\tilde{H} \propto -\boldsymbol{\sigma} \cdot \boldsymbol{k}$

Two flat bands at one graphene valley (K or K'):

Nonzero total helicity $\eta_{\text{tot}} = \pm 2$

Indicating a ***fragile topology*** *(no 2-band tight-binding model at one valley).*

Po et. al. (2018), Song et al. (2018)

Outline

***Twisted bilayer graphene (TBG)**:*

- *Flat bands, Dirac helicity*
- *Moire electron-phonon coupling*
- *BCS superconductivity & implication on insulator states*

Superconductor & Interacting insulator

Interacting insulator phases & superconductivity observed near the magic angle:

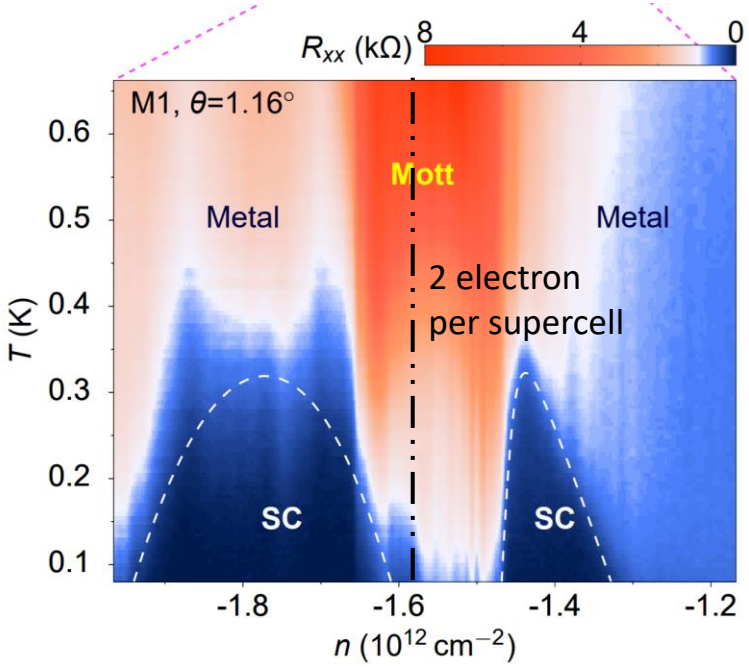

Cao et. al. (2018)

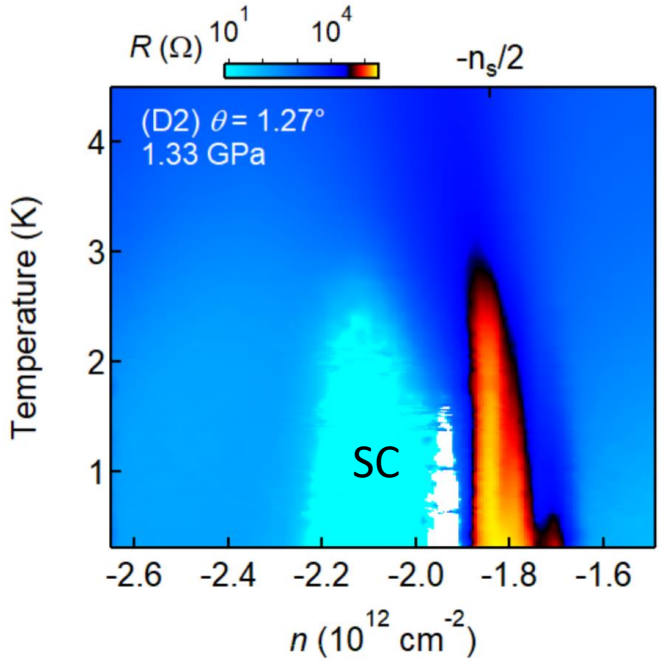

TBG under pressure, Yankowitz et. al. (2018)

BCS superconductivity (phonon)?

Wu, MacDonald, Martin (2018), Lian, Wang, Bernevig (2018),
Choi, Choi (2018), Wu, Hwang, Das Sarma (2018)

Moire enhanced electron-phonon coupling

The Moire pattern enhances the electron-phonon coupling.

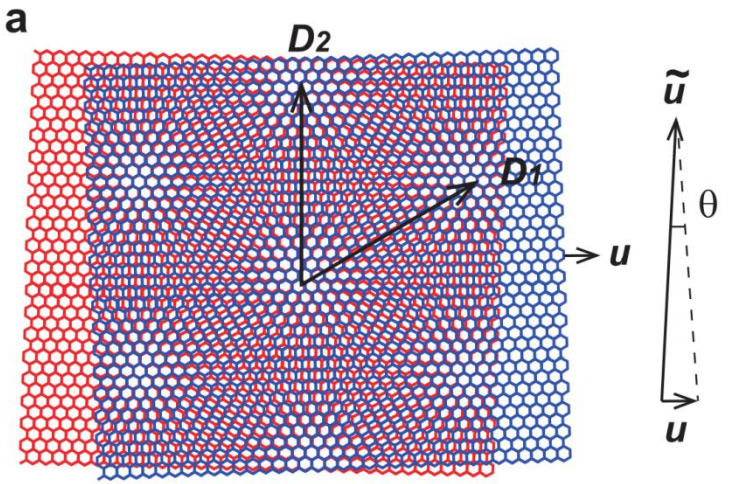

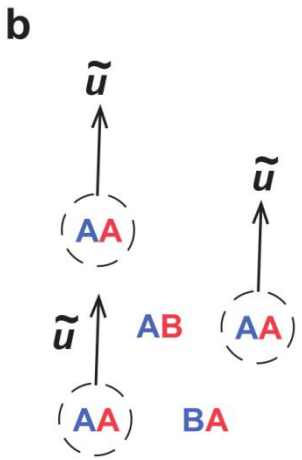

$$\boldsymbol{u} = \boldsymbol{u}_1 - \boldsymbol{u}_2$$

The relative in-plane displacement $\boldsymbol{u}$ (phonon field) between layers gives an ***amplified*** displacement of the Moire pattern:

$$\tilde{\boldsymbol{u}} = \gamma \hat{\boldsymbol{z}} \times \boldsymbol{u}, \qquad \gamma = \frac{1}{2\tan\theta/2} \gg 1\,.$$

Moire enhanced electron-phonon coupling

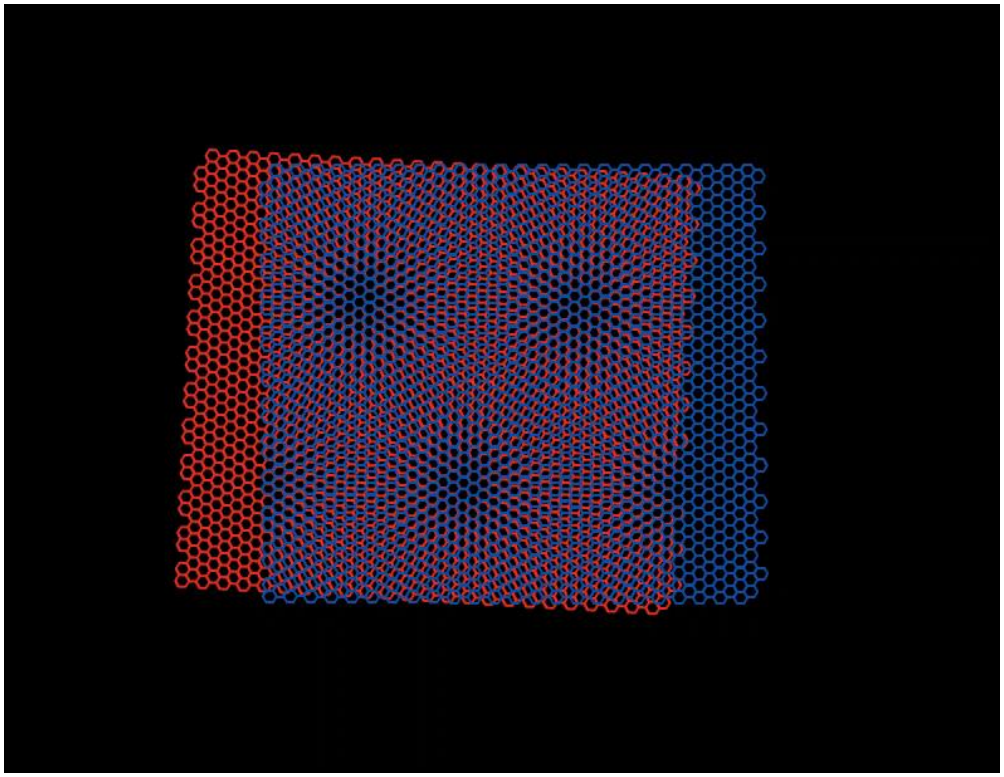

Effect of interlayer rotation, expansion and shear

In-plane interlayer phonon field $\boldsymbol{u}$ strongly affects the Moire potential, yielding ***enhanced electron-phonon couplings***.

Computing electron-phonon coupling

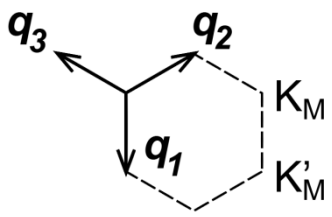

Moiré BZ

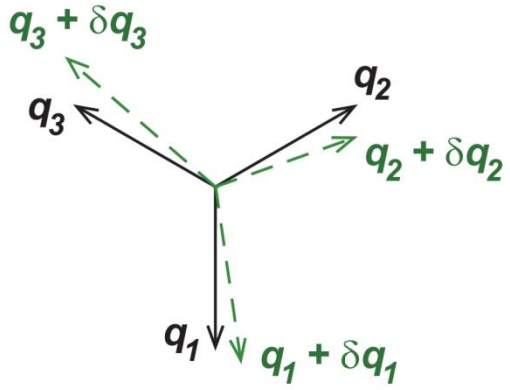

k space deformation

$$\delta\mathbf{q}_1 = \gamma k_\theta(\partial_x u_x, \partial_y u_x),$$

$$\delta\mathbf{q}_{2,3} = \cdots$$

Computing *electron-phonon (long wavelength) coupling* :

deforming $\boldsymbol{q}_j \to \boldsymbol{q}_j + \delta\boldsymbol{q}_j$ in the electron Hamiltonian:

$$H^K(\boldsymbol{r}) = \begin{pmatrix} h^K_{\theta/2}(-i\nabla) & w(T_1 e^{i\boldsymbol{q}_1\cdot\boldsymbol{r}} + T_2 e^{i\boldsymbol{q}_2\cdot\boldsymbol{r}} + T_3 e^{i\boldsymbol{q}_3\cdot\boldsymbol{r}}) \\ w(T_1 e^{-i\boldsymbol{q}_1\cdot\boldsymbol{r}} + T_2 e^{-i\boldsymbol{q}_2\cdot\boldsymbol{r}} + T_3 e^{-i\boldsymbol{q}_3\cdot\boldsymbol{r}}) & h^K_{-\theta/2}(-i\nabla) \end{pmatrix}$$

$$\boldsymbol{q}_j + \delta\boldsymbol{q}_j$$

Electron-phonon coupling: $\delta H^K(\boldsymbol{r}) \propto \partial\boldsymbol{u}$

Computing electron-phonon coupling

Electron-phonon coupling near the flat band Dirac points:

graphene valley $\eta = \pm 1\ (K, K')$, *Moire valley* $\zeta = \pm 1\ (K_M, K'_M)$, *spin* $s = \pm 1\ (\uparrow, \downarrow)$

$$H_{\rm ep}^{\eta,\zeta,s}(\overline{\mathbf{k}}) = H_{C3}^{\eta,\zeta,s}(\overline{\mathbf{k}}) + H_{\rm SO(2)}^{\eta,\zeta,s}(\overline{\mathbf{k}}) \ , \qquad \overline{\boldsymbol{k}} = \frac{\boldsymbol{k}+\boldsymbol{k}'}{2}$$

$$\begin{cases} H_{C3}^{\eta,\zeta,s}(\overline{\mathbf{k}}) = g_{1\alpha}\eta\gamma\hbar v\psi^\dagger_{\mathbf{k}'}[\overline{k}_x(\partial_y u_x + \partial_x u_y) + \overline{k}_y(\partial_x u_x - \partial_y u_y)]\psi_{\mathbf{k}} \ , \\ H_{\rm SO(2)}^{\eta,\zeta,s}(\overline{\mathbf{k}}) = \gamma\hbar v\psi^\dagger_{\mathbf{k}'}[g_{2\alpha}(\eta\sigma_x\overline{k}_x - \sigma_y\overline{k}_y)(\partial_y u_x - \partial_x u_y) \\ \qquad + g_{3\alpha}(\eta\sigma_x\overline{k}_y + \sigma_y\overline{k}_x)(\partial_x u_x + \partial_y u_y)]\psi_{\mathbf{k}} \ , \end{cases}$$

$$g_{1\alpha} = \frac{9\alpha^2(1+3\alpha^2)}{(1+6\alpha^2)^2} \qquad g_{2\alpha} = \frac{9\alpha^2}{(1+6\alpha^2)^2} \qquad g_{3\alpha} = \frac{3\alpha^2}{1+6\alpha^2}$$

The e-p coupling (long wavelength) only depends on graphene valley η (Dirac helicity).

Phonon Hamiltonian

Interlayer coupling of in-plane phonons is ***negligible***.

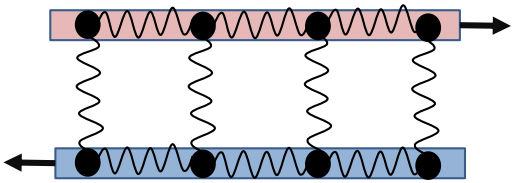

Bilayer sideview

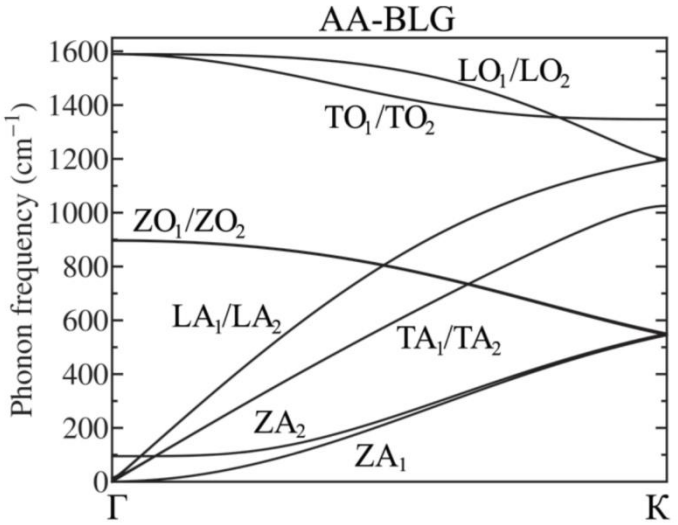

Phonon spectrum of AB BLG

Cocemasov, Nika, Balandin (2013)

In-plane interlayer phonons (acoustic):

$$H_{\rm ph} = \sum_{\mathbf{p}} \left(\hbar\omega_{\mathbf{p},L} a^{\dagger}_{\mathbf{p},L} a_{\mathbf{p},L} + \hbar\omega_{\mathbf{p},T} a^{\dagger}_{\mathbf{p},T} a_{\mathbf{p},T} \right),$$

$$\omega_{\mathbf{p},L} = c_L p \qquad \omega_{\mathbf{p},T} = c_T p$$

$c_L, c_T \sim 10^4 m/s$

Phonon field $u_{\mathbf{p},\chi} = \sqrt{\frac{\hbar\Omega}{2M\omega_{\mathbf{p},\chi}}}(a_{\mathbf{p},\chi} + a^{\dagger}_{-\mathbf{p},\chi})$ for $\chi = L, T$.

Phonon mediated interaction

Acoustic phonon induced electron interaction (BCS channel) near magic angle ($c_L \approx c_T$):

between graphene valley η & η':

$$\frac{V^{II'}_{\mathbf{k}\mathbf{k}'}(\omega)}{\Omega_s} \approx \frac{\hbar^2 v^2 k_F^2 \varpi^{\eta\eta'}_{\mathbf{k}\mathbf{k}'}}{9Mc_T^2} \frac{\omega^2_{\mathbf{p},T}}{\omega^2 - \omega^2_{\mathbf{p},T}} f_{\eta\eta'}(\varphi_{\mathbf{k}}, \varphi_{\mathbf{k}'}),$$

$$f_{\eta\eta'}(\varphi_{\mathbf{k}}, \varphi_{\mathbf{k}'}) = \begin{cases} -1 - 2\cos(\varphi_{\mathbf{k}} - \varphi_{\mathbf{k}'}), & (\eta = \eta') \\ \left| 1 - \eta \frac{e^{2i\varphi_{\mathbf{k}}} - e^{2i\varphi_{\mathbf{k}'}}}{e^{-i\varphi_{\mathbf{k}}} - e^{-i\varphi_{\mathbf{k}'}}} \right|^2 . & (\eta = -\eta') \end{cases}$$

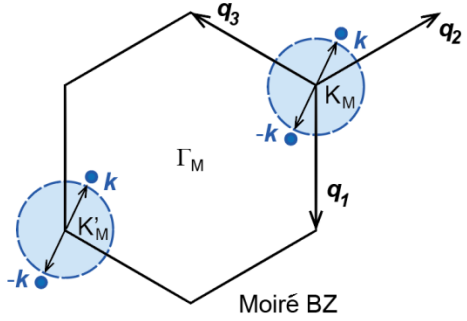

Fermi surface illustration

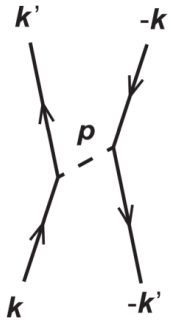

$$\varpi^{\eta\eta'}_{\mathbf{k}\mathbf{k}'} = e^{i(\frac{\eta+\eta'}{2})(\varphi_{\mathbf{k}} - \varphi_{\mathbf{k}'})} \left[\frac{1 + \cos(\varphi_{\mathbf{k}} - \varphi_{\mathbf{k}'})}{2} \right]$$

The interaction is *attractive* for intervalley ($\eta = -\eta'$), and *repulsive* for intravalley ($\eta = \eta'$).

Phonon mediated interaction

Repulsive nature of ***intravalley*** interaction:

for arbitrary intravalley 2-electron state: $E_{KK} = \langle \Psi_{KK} | H_{\text{int}}^{(\text{ph})} | \Psi_{KK} \rangle > 0$.

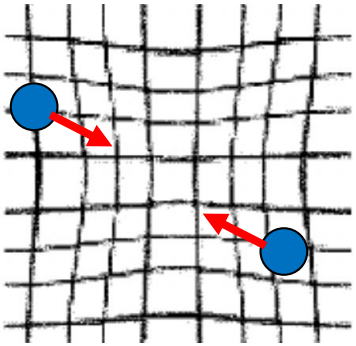

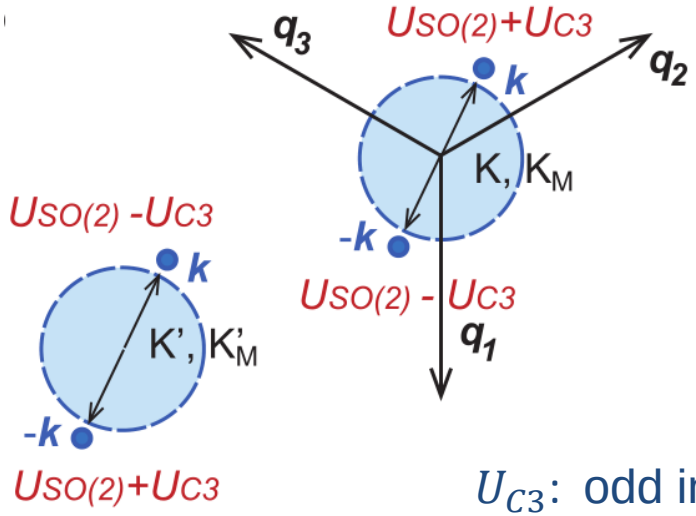

U_{C3}: odd in $\boldsymbol{k}$, odd in graphene valley

Understanding:

$$H_{\text{ep}}^{\eta,\zeta,s}(\bar{\mathbf{k}}) = \underbrace{H_{C3}^{\eta,\zeta,s}(\bar{\mathbf{k}})}_{U_{C3}} + \underbrace{H_{\text{SO}(2)}^{\eta,\zeta,s}(\bar{\mathbf{k}})}_{U_{SO(2)}} ,$$

Lattice potential: $U_{C3} > U_{SO(2)}$

Mediated interaction

$$\propto \pm U_{C3}^2 - U_{SO(2)}^2 .$$

Outline

***Twisted bilayer graphene (TBG)**:*

- *Flat bands, Dirac helicity*
- *Moire electron-phonon coupling*
- *BCS superconductivity & implication on insulator states*

Coulomb interaction

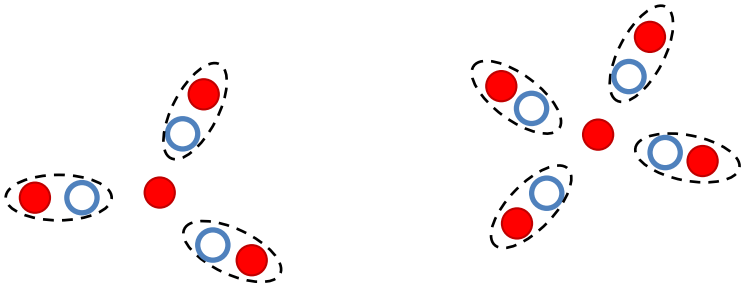

$$\epsilon(q) \approx \epsilon_I \left(1 + \frac{q_{\mathrm{TF}}}{q}\right)$$

Large density of states (DoS) N_D of the flat bands strongly screens the Coulomb interaction.

Thomas-Fermi approximation (2D):

TF momentum $q_{\mathrm{TF}} = 2\pi e^2(\partial n_e/\partial\mu)/\epsilon_I = 2\pi e^2 N_D/\epsilon_I \gg q$

→ *Coulomb repulsion*: $\mathcal{V}_e(q) \approx 2\pi e^2/\epsilon_I q_{TF} \sim N_D^{-1}$

→ *In large DoS limit, the Coulomb coupling strength* $\mu_c = N_D \mathcal{V}_e(q) \approx 1$.

Coulomb interaction

Near magic angle, the DoS $N_D \geq 1\, meV^{-1} \cdot \Omega_s^{-1}$, ($\Omega_s$: supercell area)

→ Screened Coulomb interaction

$$\mathcal{V}_e(q)/\Omega_s \leq 1\, meV\ .$$

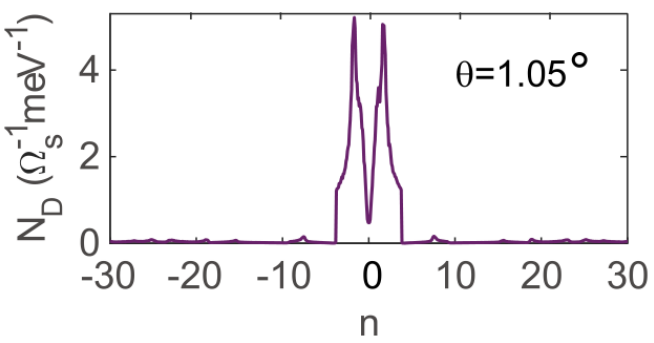

Acoustic phonon mediated intervalley attraction:

$$V_{\boldsymbol{kk'}}^{KK'}(\omega = 0)/\Omega_s \sim -1meV\ .$$

→ Strong BCS coupling strength $\lambda \sim -N_D V_{\boldsymbol{kk'}}^{KK'} \geq 1$.

(*Optical phonon may further contribute: future study*)

BCS superconductivity

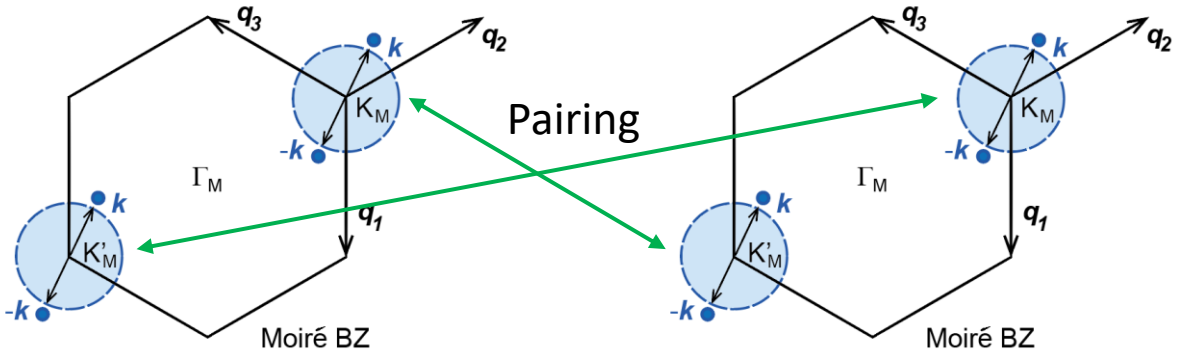

Graphene valley K Graphene valley K'

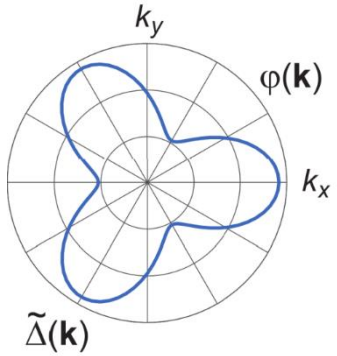

Pairing $\Delta(\eta \boldsymbol{k})$

This favors an **intervalley *s*-wave** BCS superconductivity, with a strong BCS coupling strength $\lambda \geq 1$ (*spin singlet-triplet degenerate*).

McMillan formula $T_c = \dfrac{\hbar\omega_D}{1.45k_B}\exp\left[-\dfrac{1.04(1+\lambda)}{\lambda-\mu_c^*(1+0.62\lambda)}\right]$, $\mu_c^* = \mu_c/[1+\mu_c\ln(\omega_{pe}/\omega_D)]$

Debye (acoustic) $\hbar\omega_D \sim \hbar c_T k_\theta \sim 2meV$, *Coulomb* $\mu_c \sim 1$, $\dfrac{\omega_{pe}}{\omega_D} \sim 10$

$\lambda = 1.5 \rightarrow T_c \sim 1K$. $\lambda = 1 \rightarrow T_c \sim 0.3K$.

Apply to other angles & fillings

Electron-phonon coupling at other angles & fillings (numerical):

Under $\boldsymbol{q}_j \to \boldsymbol{q}_j + \delta\boldsymbol{q}_j$ *, the band energy change* $\delta H(\boldsymbol{k}) \sim b(\boldsymbol{k})\partial_i \boldsymbol{u}_j$

→ *phonon-mediated interaction in higher bands.*

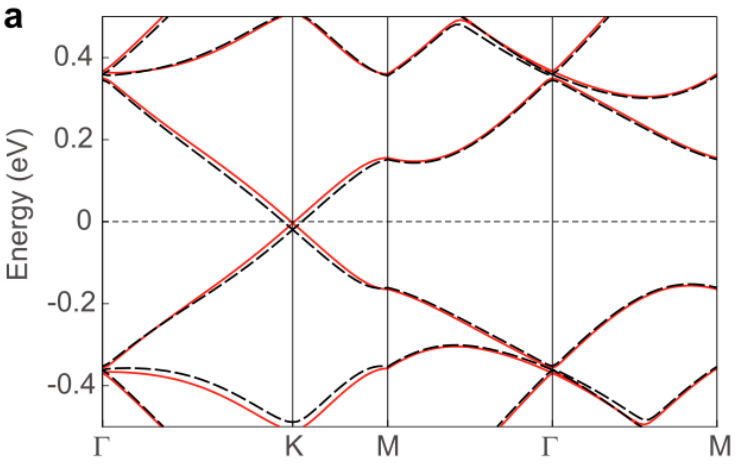

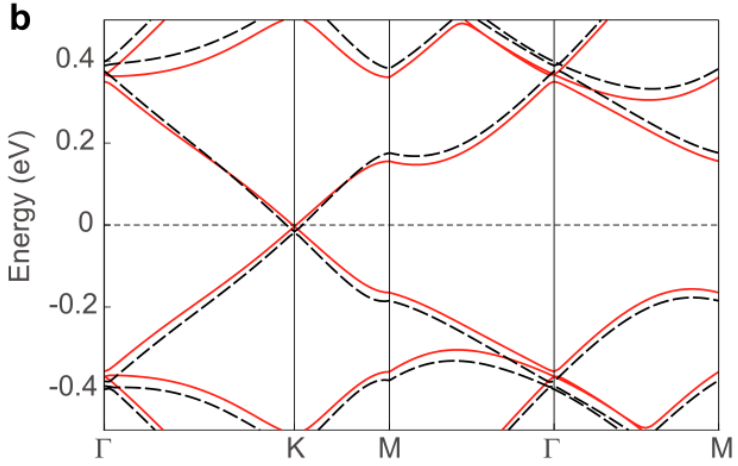

$\delta H(\boldsymbol{k})$ in continuum model

$\delta H(\boldsymbol{k})$ in *ab initio (commensurate deform)*

Deformation $\partial_i u_j \sim 0.01$ $(\theta = 3.15°)$

ab initio with commensurate deformation

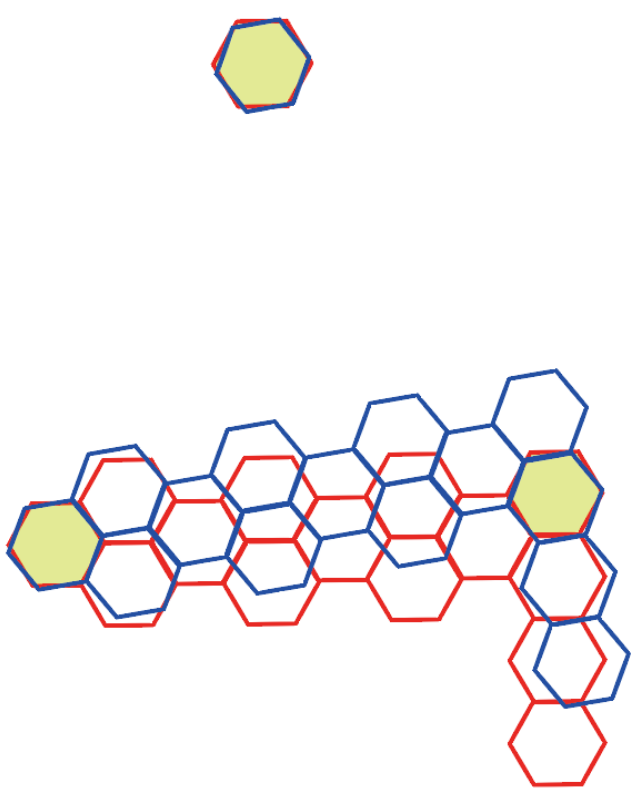

TBG before deformation

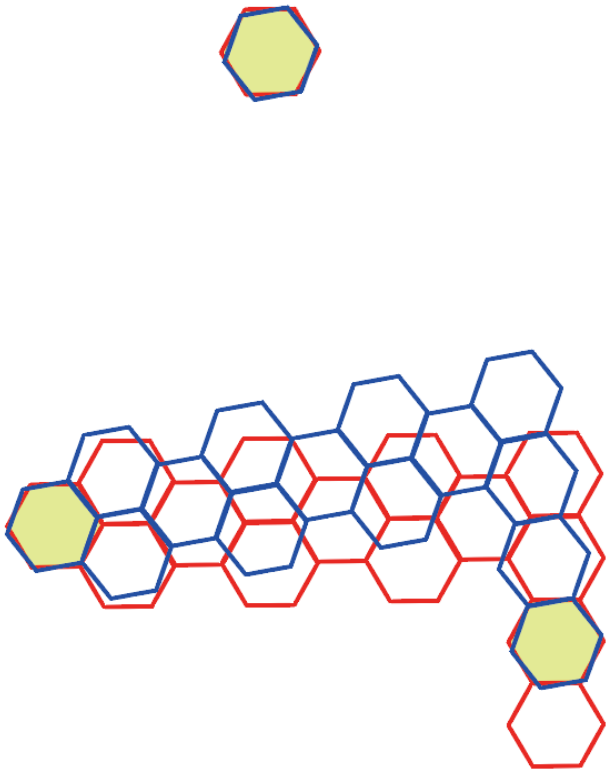

TBG after deformation

BCS at other angles & fillings

Moire pattern also enhances electron-phonon coupling in higher bands (large band width).

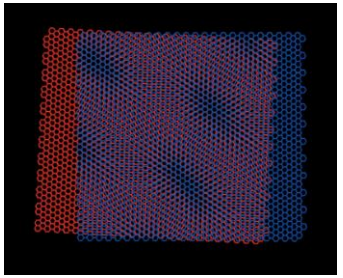

Tc of TBG in McMillan formula (if BCS superconductivity):

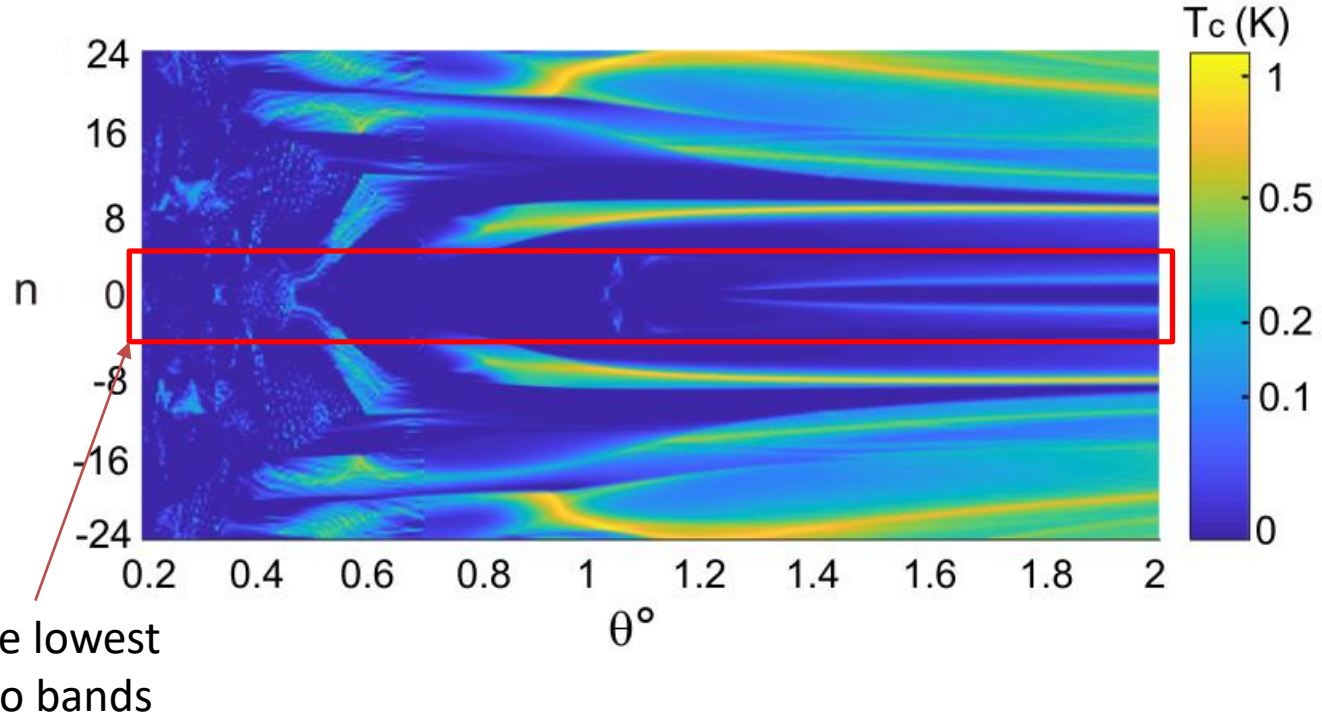

BCS coupling at higher fillings

DoS

BCS coupling

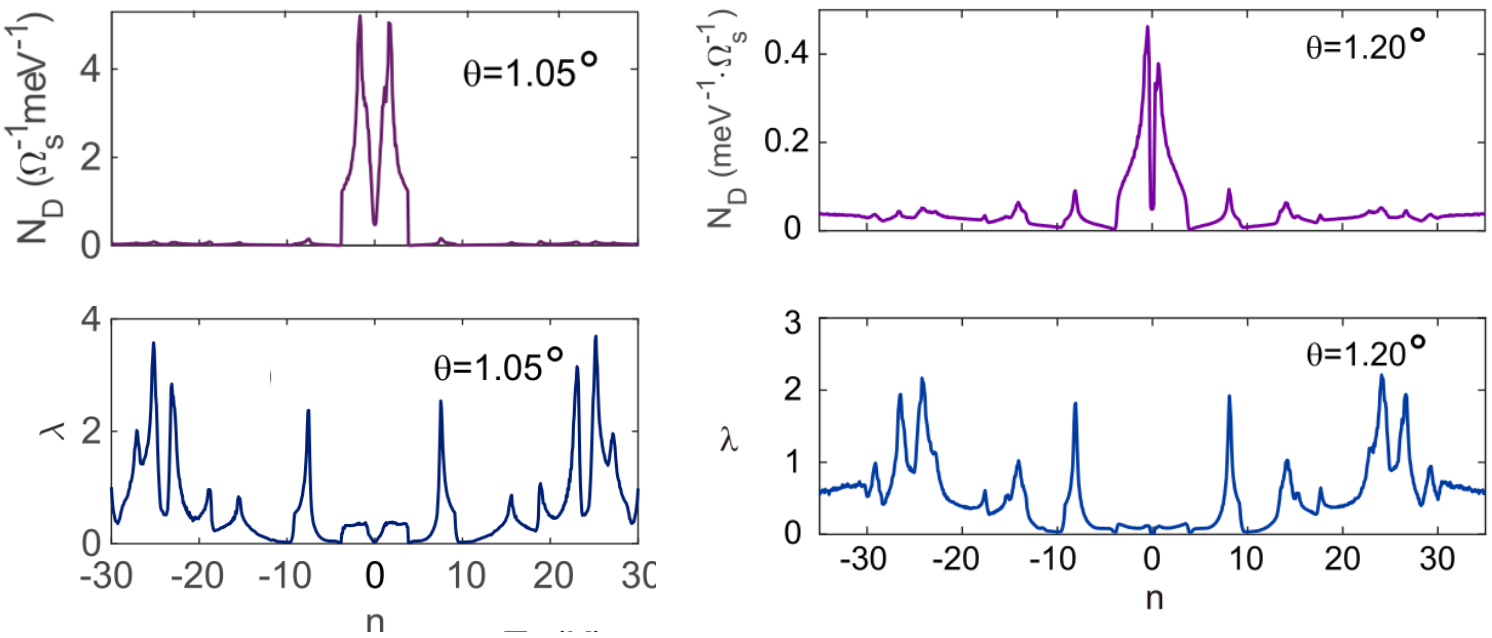

Strong phonon-mediated interaction may also induce ***charge density waves, etc,*** instead of ***superconductivity***.

Implication for insulator phases

Insulator phases are observed at quarter fillings (1, 2, 3 electrons per supercell)

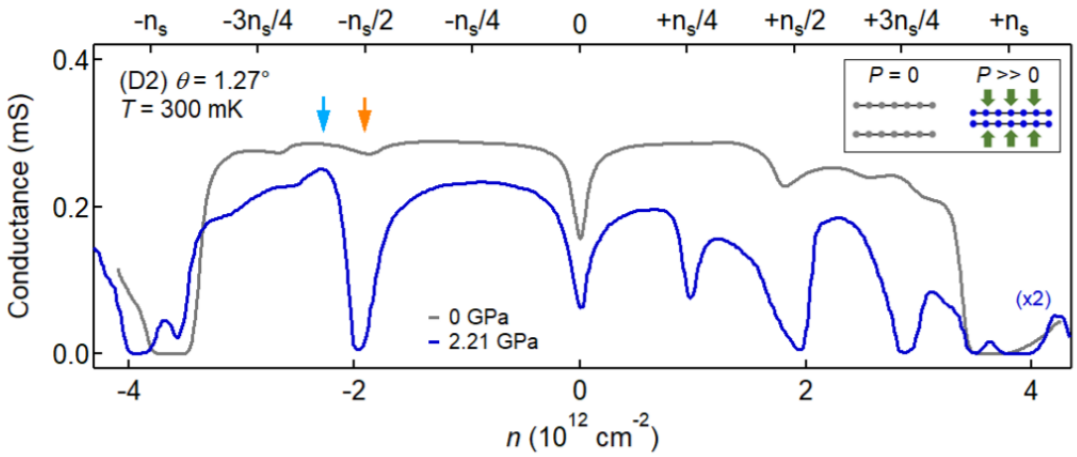

Local interaction (spin s, graphene valley η)

$$V \sim \sum_{s,s',\eta,\eta'} (V_0 + \eta\eta' V_1) n_{s,\eta} n_{s',\eta'},$$

V_0: screened Coulomb, V_1 : phonon.

V_1 *breaks the SU(4) symmetry* among spin & graphene valley.

Cao et. al. (2018), Yankowitz et. al. (2018), Sharpe et. al. (2019)

Analogy to Bose Mott insulator

$$V \sim \sum_{s,s',\eta,\eta'} (V_0 + \eta\eta' V_1) n_{s,\eta} n_{s',\eta'}$$

If BCS superconductivity, one could have $V_1 > V_0$ or comparable.

Bose Mott insulator of Cooper pairs?

Expected Feature: superconductor-insulator transition resistivity (isotropic) at

$$\rho \approx \frac{h}{(2e)^2} \approx 6k\Omega \ .$$

Charge density wave (anisotropic)?

Fisher, Weichman, Grinstein, Fisher (1989), Yazdani, Kapitulnik (1995)

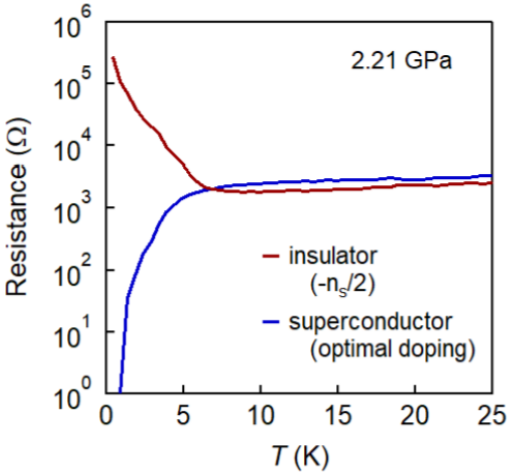

TBG resistance
Yankowitz et. al. (2018)

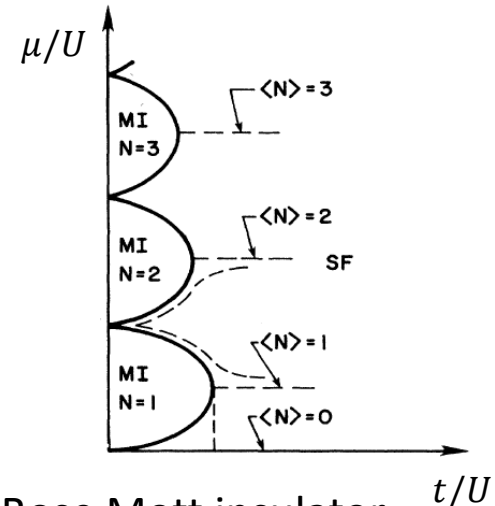

Bose Mott insulator

Nematicity favored by phonon

$$V \sim \sum_{s,s',\eta,\eta'} (V_0 + \eta\eta' V_1) n_{s,\eta} n_{s',\eta'}$$

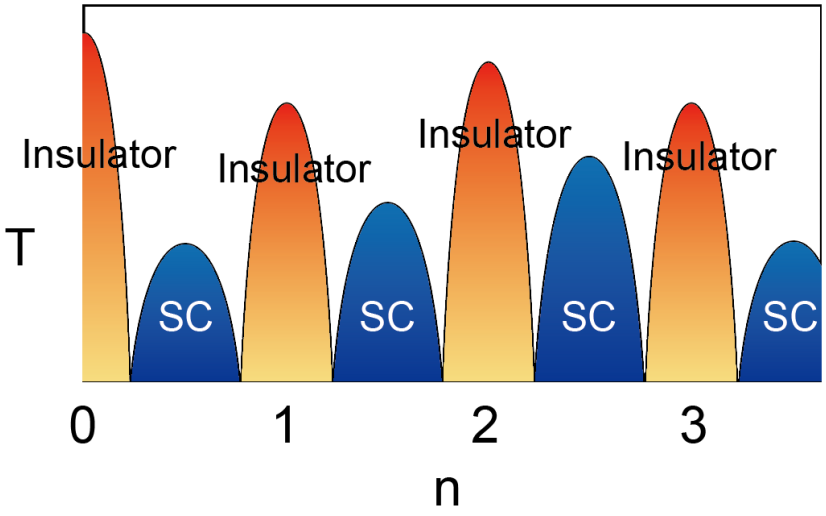

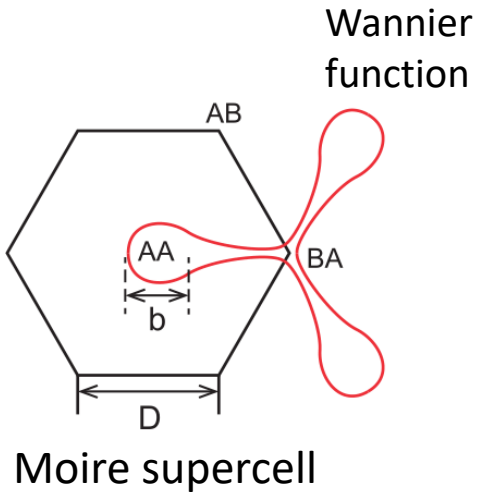

- Delocalized Wannier ($V_1 = 0$): → Nematic insulator at $n = 1$ & 3 .

Kang, Vafek (2018)

- Delocalized Wannier + Phonon-mediated V_1 favors ***valley nematicity*** at all integer n insulators → *nematic SC (unpublished)*

Nematic insulator pattern (unpublished)

$\pm$: graphene valley index

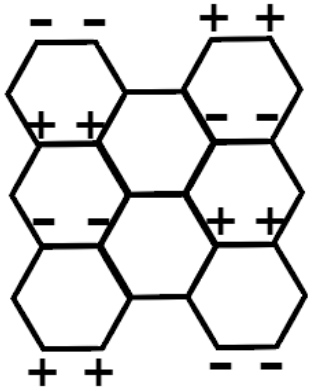

$U_1 > U_0$

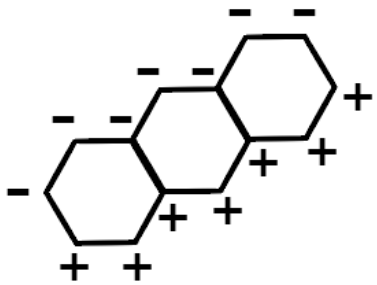

$U_1 > \alpha_1^2 U_0$,
$\alpha_1 \sim 0.2$

$n = 2$ electrons per supercell

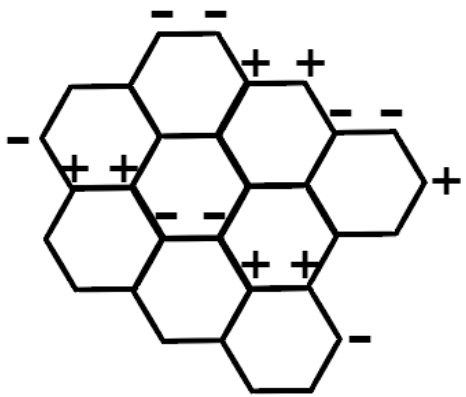

$U_1 < U_0$

$n = 1$ electrons per supercell

Summary

- The (generic) Moire pattern enhances the interlayer phonon-electron coupling.
- Phonon (acoustic) mediated electron interaction in TBG favors a intervalley pairing.
- Superconductivity in TBG can exist in higher bands & other angles.
- Insulating states: Bose Mott insulator analogy, nematicity.
- Electron-phonon coupling in other Moire systems (ABC/hBN trilayer, double bilayer graphene, TMDC)?